BMC Cancer

RESEARCH Open Access

Potential changes in microorganisms and metabolites associated with oral cancer: a preliminary study

Kaitong Wei[1†], Yaqing Ma[1†], Jing Xu[1†], Hongyu Zheng[1,3], Lianping Xue[2], Yaojuan Chu[2], Yingying Shi[2], Zhi Sun[2] and Qiang Sun[1*]

Abstract

Background Oral squamous cell carcinoma is a malignant tumor with high morbidity and mortality, and changes in microflora have a close relationship with tumor development. In this study, we tried to identify the changes in oral microbial characteristics and metabolite levels in OSCC patients.

Methods In this study, saliva samples were collected from 40 oral cancer cases and 39 healthy controls. The microbiome was analysed by 16 S rDNA gene sequencing, and the metabolome was detected by Liquid Chromatography-Mass Spectrometry (LC-MS) with metabolite traceability using the Metorigin platform. Correlations between the microbiome and metabolome were analysed using the Spearman correlation method.

Results The study found a significant difference in the β diversity of oral microbiota between the oral cancer group and healthy controls, while α diversity showed no significant difference. At the phylum level, Deferribacterota significantly increased, and Cyanobacteria significantly decreased in the oral cancer group. At the genus level, Vibrio and Lactococcus were significantly elevated, while Bifidobacterium and Faecalibacterium were significantly reduced. Metabolomic analysis identified 36 differentially abundant metabolites; 13(S)-HOTrE and 13-HODE were significantly downregulated, while docosanamide was significantly upregulated in the oral cancer group. Six bacteria-specific metabolites, including Indole, were also downregulated. Correlation analysis showed that N-Acetylneuraminic acid had a significant negative correlation with Pseudoalteromonas and Vibrio ($r < -0.4$).

Conclusion This study found large differences in microbiome levels at the portal level, at the genus level, and significant differences in the levels of a variety of metabolites labeled by indoles, providing a new and potentially valuable direction for the diagnosis and treatment of oral squamous carcinoma.

Keywords Oral squamous cell carcinoma, Microbiome, Metabolites, Diagnostic markers, Oral microenvironment

†Kaitong Wei, Yaqing Ma and Jing Xu contributed equally to this work.

*Correspondence:
Qiang Sun
fccsunq1@zzu.edu.cn

[1]Oral and Maxillofacial Surgery, The First Affiliated Hospital of Zhengzhou University, Zhengzhou, Henan Province 450052, China
[2]Department of Pharmacy, The First Affiliated Hospital of Zhengzhou University, Zhengzhou, Henan Province 450052, China
[3]The First Affiliated Hospital of Chongqing Medical University, Chongqing, China

Background

Oral malignancies are among the most common malignancies of the head and neck, and according to Globocan 2022, oral cancer ranks 16th in global cancer incidence, accounting for 1.95% of all cancer cases, and 15th in mortality, accounting for 1.93% of all cancer cases worldwide, about 90 per cent of them are oral squamous cell carcinoma (OSCC) [1–3]. Recognised causes of oral cancer include smoking, alcohol consumption, poor oral hygiene, human papillomavirus (HPV) infection and betel nut consumption [4–7]. In addition, there is growing evidence linking the human oral microbiota to the development of oral cancer [8, 9].

Microorganisms play a role in cancer development and progression [10, 11]. Studies have confirmed a strong correlation between oral periodontal pathogens and malignancy, particularly *Porphyromonas gingivalis*, *Clostridium nucleatum* and *Spirochaetes denticolais* [12–14]. Among fungi, *Candida* is strongly associated with oral cancer [15]. Numerous studies have shown that *viral HPV* is a risk factor for oropharyngeal squamous cell carcinoma, especially high-risk hpv16 [16], which may promote tumorigenesis by enhancing epithelial cell proliferation, inhibiting apoptosis, and modulating the inflammatory microenvironment. However, the role of the oral microbiota in oral squamous cell carcinoma is unclear.

Microbial metabolic activity is considered an important bridge between the microbiota, the tumor microenvironment and cancer development [17, 18]. In addition, malodour often occurs in the mouths of patients with oral malignancies [19]. These pungent odours are formed by volatile compounds, which are produced mainly by anaerobic bacteria through their metabolic activities, including volatile sulphur compounds, aromatic compounds, amines, and short-chain fatty acids [20]. Accordingly, it can be hypothesised that the microbiome and its metabolic activities may play important roles in the development and progression of oral cancer.

Salivary metabolomics is a rapidly growing discipline that aims to provide real-time molecular phenotypes reflecting oral health [21, 22]. Metabolic reorganisation is a hallmark of cancer and may serve as a diagnostic and therapeutic target [23, 24]. Unlike other deeply invasive cancers, oral cancer is located in the oral cavity in direct contact with saliva, and saliva sampling may be an effective method for identifying sensitive and specific biomarkers for this disease [25, 26].

This study aims to explore the combination of characteristic changes in oral cancer-related microbiomics and metabolomics, which can effectively provide new perspectives on the effects of oral cancer on organisms and provide an experimental basis for further exploration of the potential mechanisms of the bacterial microbiome involved in oral carcinogenesis.

Methods

Study participants

From August 2022 to May 2023, we recruited 40 patients with OSCC and 39 healthy participants at the First Affiliated Hospital of Zhengzhou University, all of whom provided informed consent and complete clinical and pathological information. The study was approved by the Ethics Committee of the First Affiliated Hospital of Zhengzhou University (Ethics Approval: 2019-KY-305).

The inclusion criteria for the OSCC group were patients who underwent pathological biopsy of OSCC, patients without severe periodontal disease, severe caries or other serious oral diseases, patients with other systemic diseases, patients with no history of surgery, patients with no history of antibiotic application, and patients with no history of radiotherapy in the 3 months prior to enrollment.

The OSCC exclusion criteria for patients were as follows: history of oral infectious diseases or bleeding, history of antibiotic use within 3 months prior to enrolment, and history of other systemic diseases.

Healthy participants who had not used antibiotics within 3 months; had no severe periodontal disease, severe caries, or other serious oral disease; and had no personal or family history of autoimmune disease or other serious systemic disease were included in the HC (healthy control) group.

Sample collection

In accordance with the method of saliva collection from OSCC patients adopted by Nikolay [27] et al., the collection time ranged from 8 a.m. to 9 a.m. Each participant was asked to refrain from smoking, drinking, and eating for at least 1 h prior to sample collection. The mouth was rinsed twice with distilled water, and participants were asked to gently hold the tip of the tongue against the lingual side of the palate or mandibular incisors to enrich the saliva, which was then gently spat into a centrifuge tube until the liquid saliva (nonbubbly) reached the 5 ml mark. The mixture was centrifuged at 4 °C and 3000 rpm(279.5 g) for 10 min, and the supernatant was dispensed into new EP tubes. Immediately after coding, the samples were stored in an ultralow temperature refrigerator (-80 °C) for backup.

DNA extraction and 16 S rDNA sequencing of saliva samples

Microbial genomic DNA was extracted from saliva samples via the cetyltrimethyl ammonium bromide (CTAB) method, and the DNA concentration was determined via NanoDrop One, and the purity was determined via

1% agarose gel electrophoresis. The DNA was diluted to 1 ng/μl, and the 16 S rDNA of the V3-V4 region was amplified with the primers 341 F and 805R. The PCR products were purified from AMPure XT beads (Beckman Coulter Genomics, Danvers, MA, USA) and quantified with a Qubit instrument (Invitrogen, USA), and the PCR-amplified products were detected via 2% agarose gel electrophoresis. An AMPureXT bead recovery kit (Beckman, USA) was used. The purified PCR products were evaluated via an Agilent 2100 Bioanalyzer (Agilent, USA) and an Illumina Kapa Biosciences (Woburn, MA, USA) library quantification kit. The qualified libraries for each upsequencing (index sequences are not reproducible) were diluted in a gradient, mixed at the appropriate ratio according to the required sequencing volume, and denatured by NaOH to single-stranded for upsequencing; 2 × 250 bp bipartite sequencing was carried out via the NovaSeq 6000 Sequencer (Illumina, USA) and the corresponding reagent NovaSeq 6000 SPReagent Kit (Illumina, USA).

LC–MS analysis and data collection

Chromatographic separation was achieved via a Dionex Ultra 3000 liquid chromatograph (Thermo Scientific, San Jose, USA). Gradient elution was used, with mobile phase A being acetonitrile and mobile phase B being water containing 0.1% formic acid. The chromatographic column used was an ACQUITY UPLC BEH C18 column (2.1 mm×100 mm, 1.7 μm, Waters, USA). The injection volume was 5 μL, the column temperature was 40 °C, and the flow rate was 0.350 m L/m. The chromatograph was interfaced with a Q Exactive Orbitrap mass spectrometer (Thermo Fisher Scientific, San Jose, USA). The instrument was scanned over a mass range of 80–1200 m/z, with an ion source temperature of 350 °C, a capillary temperature of 320 °C, collision energies of 20, 40, and 60 eV, and spray voltages of + 3.50 or -2.8 kV. Mass spectra were obtained by full MS/ddms^2 operating in positive and negative ion modes. scanning modes to obtain mass spectra. To assess both reproducibility and stability during the run, quality control (QC) samples were obtained by mixing all saliva samples separately, and the QC samples followed the same procedure as the test samples. The experimental samples were randomised during the run, with QC samples injected every eight samples, and mixed standard solutions were analysed in the same way as the biological samples. Mass spectrograms and spectral data were recorded via Xcalbur software (Thermo Fisher Scientific, USA). Metabolites were extracted from the raw data via Compound Discoverer software (version 2.1). The resulting comprehensive peak list (molecular weight, retention time, peak area) was derived for subsequent statistical analysis and metabolomics visualisation.

Bioinformatics analysis, statistical analysis and visualisation

For 16 S rDNA gene sequencing analysis, α and β diversity values were calculated via the Quantitative Insights Into Microbial Ecology (QIIME) toolkit (version 2.0) [28]. After the operational taxonomic unit (OTU) table was refined,α diversity [29] was used to calculate taxa richness and evenness within bacterial populations via metrics such as the Chao1, observed taxa, Good's coverage, Shannon, Simpson and Pielou indices. The Wilcoxon paired signed rank test was used to calculate the significance of the α diversity indicators. The heterogeneity of the microbial communities, i.e., β diversity, was determined via a Jaccard distance matrix calculated via the QIIME script, and its significance was also determined via analysis of similarity (ANOSIM) and aligned multivariate analysis of variance (ADONIS). The greater the Jaccard distance was, the less similar the microbial communities were. Principal coordinate analysis (PCoA) was used to visualise differences in microbial distribution between individuals and/or groups [30]. Linear discriminant analysis of effects (LEfSe) was used to statistically analyse the relative abundance of oral microbial phyla and genera in the two groups of samples [31]. Only colonies that satisfied both a linear discriminant analysis (LDA) value greater than 3 and a P value less than 0.05 with a P value of less than 0.05 by Wilcoxon Rank-Sum test were considered significantly enriched.

For metabolomics data analysis, one-way statistical analysis was used to screen for metabolites with *P* values < 0.05 and |log2(fold change (FC))| ≥ 1. Multivariate statistical analyses, including principal component analysis (PCA) and orthogonal partial least squares discriminant analysis (OPLSDA), were performed via SIMCA software (version 14.0). Ranking analysis was used to assess the reliability of the OPLSDA model, and differentiated metabolites with variable importance in projection (VIP, variable importance in projection) > 1 were selected. References were made to the MassBank (http://www.massbank.jp/), Kyoto Encyclopedia of Genes and Genomes (KEGG) (http://www.genome.jp/KEGG/), ChemSpider (http://www.chemspider.com/), Human Metabolome Database (HMDB) (http://www.hmdb.ca/) and other databases to identify potential biomarkers. The identified metabolites were further validated with reference standards on the basis of accurate mass, MS2 fragmentation and retention time. In addition, we used the in-depth analysis mode of the official Metorigin website (https://metorigin.met-bioinformatics.cn/) for metabolite traceability analysis, functional analysis and Sankey network analysis and combined the microbiological data on the platform where the metabolites differing between the two groups were subjected to bacterial colony Spearman correlation analysis. Finally, the relationships between

the differential microbiome and metabolites and the clinical characteristics of the OSCC patients were analysed via the Spearman method.

Results

Analysis of basic demographic data

Outlier samples between the two groups were identified via principal component analysis (PCA), which were excluded because their positions in the PCA plots significantly deviated from those of the other samples, which might affect the overall analysis results. After these outlier samples were removed, the cluster analysis results of the metabolism group data were more consistent, which enhanced the reliability of the results. The study included 36 patients with OSCC and 34 healthy volunteers, and there were no significant differences in sex, age, weight, height, or body mass index (BMI) between the two groups ($P > 0.05$) (Table 1).

Microbiological characteristics of saliva samples

A total of 5,816,261 high-quality sequences (83,089 sequences per sample) were obtained from the saliva samples of 70 participants (36 OSCC patients and 34 healthy controls) for sequencing. The dilution curves obtained from the Shannon and Goods coverage indices tended to be flat, indicating that the sequencing depth was deep enough to represent most of the microbial taxa for this 16 S rDNA sequencing (Fig. 1A). To assess the differences in gut microbial diversity between the OSCC and HC groups, we used six indices to detect α diversity, namely, the Chao1 index, observed taxa index, Good's coverage index, Shannon index, Simpson index, and Pielou-E index, where the Simpson index was significantly greater in the OSCC group than in the HC group ($P < 0.05$) (Fig. 1B). To further analyse the differences in microbial diversity between the two groups,β diversity analysis was performed on the data. The results of principal coordinate analysis (PCoA) based on weighted Jaccard distance and nonmetric multidimensional scaling analysis (NMDS) based on weighted UniFrac showed that there was a clear distinction between the OSCC and HC groups in terms of β diversity, and the results of Adonis and Anosim further confirmed that there was a significant difference in composition between the OSCC and HC groups (Fig. 1C).

The bacterial communities and relative abundances of the two groups were investigated at different taxonomic levels, and at the phylum level, the major phylum in the oral cavity of the OSCC group was similar to that of the HC group, consisting mainly of *Firmicutes*, *Bacteroidetes*, *Proteobacteria*, *Fusobacteriota* and *Actinobacteria*, which together comprised five phyla accounting for more than 90% of the total microbiome (Fig. 2A). At the genus level, *Streptococcus* was the most abundant genus in both the OSCC and HC groups, followed by *Neisseria*, *Veillonella*, *and Prevotella_7*. We subsequently compared the relative abundance of the OSCC group with that of the HC group at both the phylum and genus levels, and the results suggested that at the phylum level, the relative abundance of *Deferribrobacterota* was significantly greater ($P < 0.05$) than that of the HC group, whereas the relative abundance of *Cyanobacteria* was significantly lower ($P < 0.05$). At the genus level, the relative abundances of *Vibrio*, *Lactococcus*, and *Enterococcus* in the OSCC group were significantly greater ($P < 0.05$) than those in the HC group, whereas the relative abundances of *Bifidobacterium*, *Faecalibacterium*, and *Erysipelotrichaceae_UCG-003* were significantly lower ($P < 0.05$) (Fig. 2B).

To better explain the characteristic differences in microbiome between the OSCC and HC groups, we performed linear discriminant analysis effect size (LEfSe) with the screening criterion of linear discriminant analysis (LDA) > 3. The enrichment of six different categories, including phylum, order, family, genus and species, in the OSCC and HC groups is shown in Additional file 1. LEfSe analysis revealed that, at the phylum level, the content of *Campylobacterota* in the oral saliva of the OSCC group was significantly greater than that in the HC group, whereas the content of *Actinobacteria* in the oral saliva of the OSCC group was lower than that in the HC group ($P < 0.05$). At the genus level, the enrichment levels of *Catonella*, *Moraxella*, *Aggregatibacter*, and *Capnocytophaga* were significantly greater in the oral saliva of the OSCC group than in that of the HC group, whereas the abundances of the *genera Streptococcus*, *Prevotella_7*, and *Prevotella* were significantly lower ($P < 0.05$) (Fig. 2C, D). Taken together, these findings suggest a biased fitness of the oral microflora of OSCC patients.

Table 1 Demographic and other indicators for the OSCC and HC groups

Characteristic	OSCC Group ($n = 36$)	HC Group ($n = 34$)	*P*
Sex (m/f)	18/18	16/18	0.810
Age/year	57.3 ± 15.6	54.9 ± 13.4	0.469
weight/kg	65.5 ± 12.0	69.0 ± 10.6	0.280
height/cm	165.2 ± 8.7	167.1 ± 8.9	0.268
BMI	23.9 ± 3.7	24.6 ± 2.6	0.134

Metabolic characteristics of saliva samples

To ensure the stability and reliability of the metabolic profiling results, we constructed PCA score plots for all saliva samples, which revealed the intrinsic clustering of the QC samples (Fig. 3A). The relative standard deviation (RSD) distributions of the features of the QC samples revealed that more than 80% of the features had an RSD% of less than 30%, highlighting the excellent quality of the

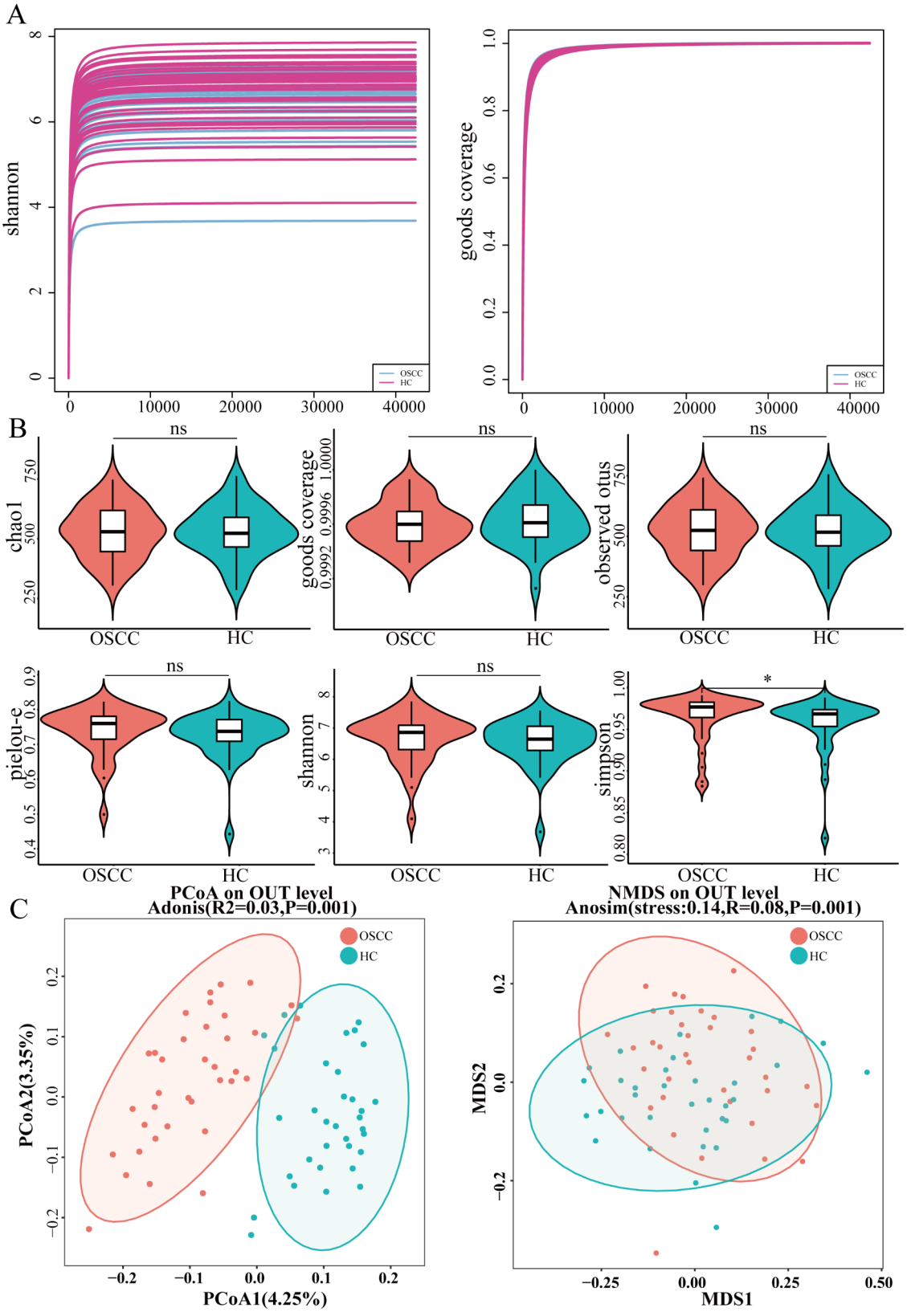

Fig. 1 Comparison of oral microbial diversity between OSCC and HC groups. **A** Sample sequencing depth of OSCC and HC groups was assessed using shannon and goods coverage indices; **B** Chao1, Observed taxa, Goods_coverage, shannon were used, Simpson and pielou-e indices to measure the α-diversity of the OSCC and HC groups. *, $P < 0.05$; **C** β diversity between the two groups calculated by principal coordinate analysis (PCoA) based on weighted Jaccard distance and non-metric multidimensional scaling analysis (NMDS) based on weighted Unifrac

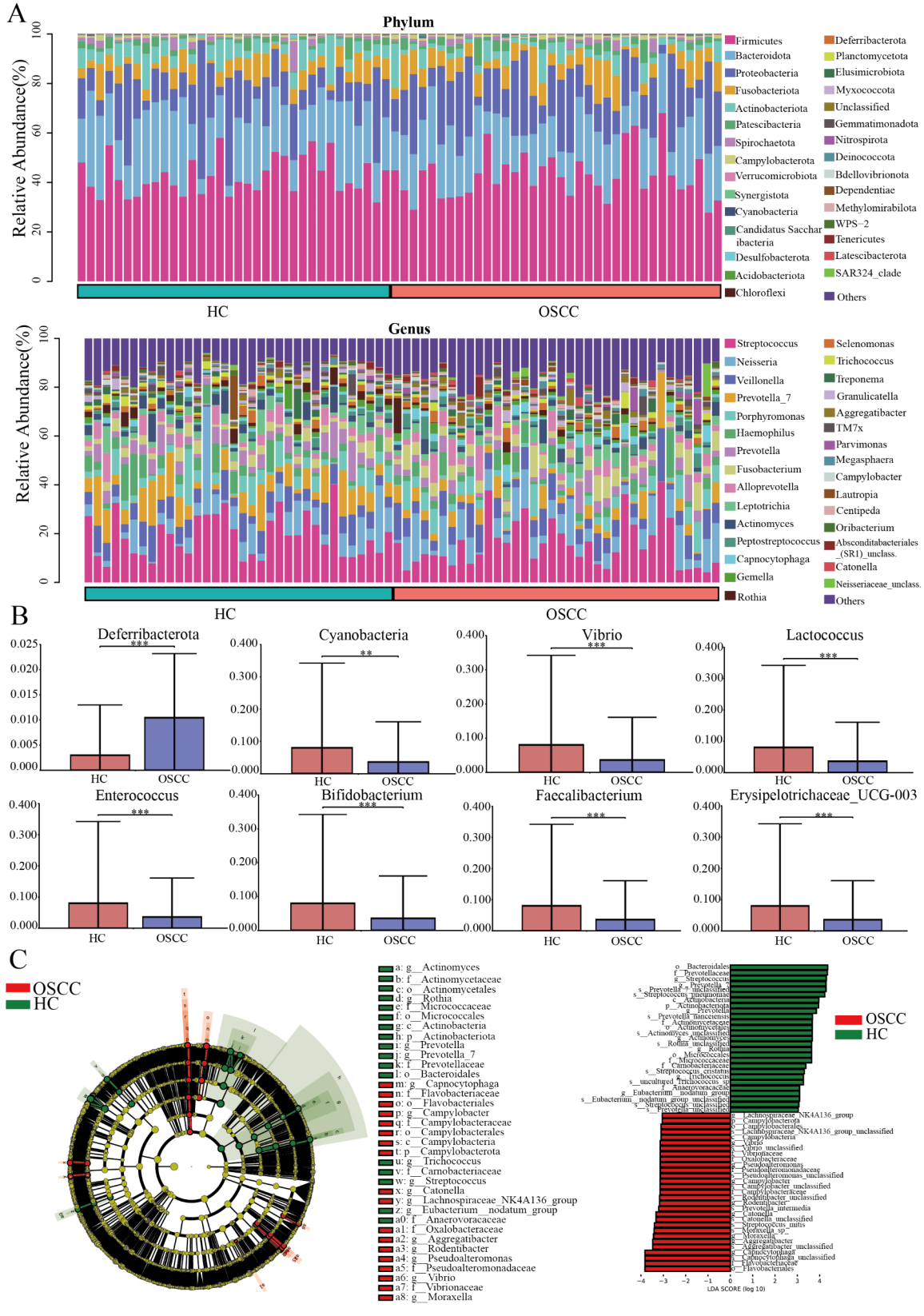

Fig. 2 (See legend on next page.)

(See figure on previous page.)

Fig. 2 Composition and abundance of oral microbiome from OSCC and HC groups. **A** histogram of relative abundance at phylum and genus levels between the two groups, showing only the top 30 phylums and the top 30 genera; **B** microbiome with significant differences in relative abundance at the phylum and genus levels. *, $P<0.05$; **, $P<0.01$; ***, $P<0.001$; **C** different circle layers in the evolutionary branching diagram on the left side radiating from the inside to the outside represent the seven taxonomic levels of phylum, phylum, family, genus and species, and the individual nodes represent the classification of a taxa at that level, and the higher the abundance, the larger the node. Yellow nodes indicate that the taxa was not significantly different between the two groups; red nodes indicate that the taxa was significantly different between the two groups and was enriched in the OSCC group; green nodes indicate that the taxa was significantly different between the two groups and was enriched in the HC group; and the linear discriminant analysis on the right side (LDA > 3, $P<0.05$) showed that the OSCC group was enriched in different levels compared with the HC group in the oral microbiome

data (Fig. 3B). The RSD values of the metabolites occurring in the QC samples were less than 30%, which can be used for the subsequent statistical analyses. In addition, the PCA plots of the samples in negative ion mode and the QC samples showed the same reproducibility (see Additional file 2), further demonstrating the robustness and validity of the data processing methods.

The data between the two groups were subjected to multivariate analyses via PCA and OPLS-DA. In the PCA score plot, we noted a trend toward differences in saliva samples between the two groups (Fig. 3C). The OPLS-DA model clearly revealed a separation between the metabolite profiles of the two groups (Fig. 3D). Ranking analysis (Fig. 3E) revealed a parameter R^2Y of 0.976 for the model's explanatory power and a parameter Q2 of 0.659 for the model's predictive power, which demonstrated that the model was reliable and free of overfitting. A total of 196 differentially abundant metabolites were identified in the positive ion model, of which 29 were upregulated and 167 were downregulated (Fig. 3F) (screening criteria $P<0.05$ and VIP > 1). A total of 71 differentially abundant metabolites were identified in the negative ion mode, of which 21 were upregulated and 50 were downregulated (see Additional file 2). A total of 40 differentially abundant metabolites were screened by multifactorial statistical analysis (screening criteria $P<0.05$ and VIP > 1) (Fig. 4 and Additional file 3). Compared with those in the HC group, 13(S)-HOTrE, (±)13-HODE and N-acetylsphingosine were significantly downregulated in the oral saliva of the OSCC group (|log2-fold change (log2FC)|>1.5, $P<0.05$), whereas 17α-methyl-androstan-3-hydroxyimine-17β-ol and docosanamide were significantly upregulated (|(log2FC)|>1, $P<0.05$).

Analysis of differences in metabolic function on the basis of metabolite source

To explore the associations between oral microorganisms and oral metabolites, we performed host-microbiome origin analysis of the differentially expressed metabolites via MetOrigin. The results suggested that the 40 differentially expressed metabolites could be categorised into 6 groups: 4 metabolites were from the host, 10 metabolites were from oral microbes, of which 6 were bacterial-specific metabolites, 12 metabolites were related to drugs, 26 metabolites were related to food, 2 were related to the environment, and 12 were unknown (Fig. 5A, B). Enrichment analysis of metabolic pathways based on metabolite source revealed two and five metabolic pathways shared by the microbiota and microbe-host, respectively, with the biosynthetic pathways of phenylalanine, tyrosine, and tryptophan in microbiota metabolism (BIO-ko00400) as well as the tryptophan metabolism pathway (BIO-ko00380) being statistically significant (hypergeometric test, log0.05) $P>1$; Fig. 5C, D). The metabolite associated with both metabolic pathways was Indole, which was significantly lower in the oral saliva of the OSCC group than in that of the HC group, and these results suggest that the rates of phenylalanine, tyrosine, and tryptophan biosynthesis and tryptophan metabolism were significantly lower in the OSCC population than in the healthy population.

The MetOrigin platform was also used to combine differentially abundant metabolites and differential microbiota for correlation analyses. Spearman correlation analysis suggested that, at the phylum level, Indole was negatively correlated with *Deferribacterota* (R=-0.43, $P<0.05$), *Cyanobacteria* was positively correlated with 13-HODE ($R=0.48$, $P<0.05$), and *Deferribacterota* was negatively correlated with a variety of metabolites (-0.6 < R<-0.4, $P<0.05$) (Fig. 6A). At the genus level, Indole was positively correlated with *Erysipelotrichaceae UCG-003*, *Collinsella*, *Clostridium sensu stricto 1*, *Faecalibacterium*, *Catenibacterium* and *Ligilactobacillus* (0.4 < R < 0.6, $P<0.05$), whereas *Erysipelotrichaceae UCG-003* was strongly positively correlated ($R>0.6$, $P<0.05$) with a variety of metabolites, including 13-HODE, and Oleoyl ethylamide Pseudoalteromonas and *Vibrio* were strongly negatively correlated (R<-0.6, $P<0.05$) with metabolites such as N-acetylsphingosine (Fig. 6B).

In addition, after integrating the correlation between biology and statistics on the MetOrigin platform, the results indicated that microbiota-specific metabolic pathways, including the tryptophan metabolism pathway (ko00380) and the biosynthesis pathway of phenylalanine, tyrosine, and tryptophan (ko00400), with an abundance of Indole, which corresponds to these two pathways, were significantly lower in the OSCC group. These findings suggest that the rates of phenylalanine, tyrosine and tryptophan biosynthesis and tryptophan metabolism were significantly lower in the OSCC group than in the HC group. Biological-Sankey (BIO-Sankey) network diagrams revealed correlations between the microbiota

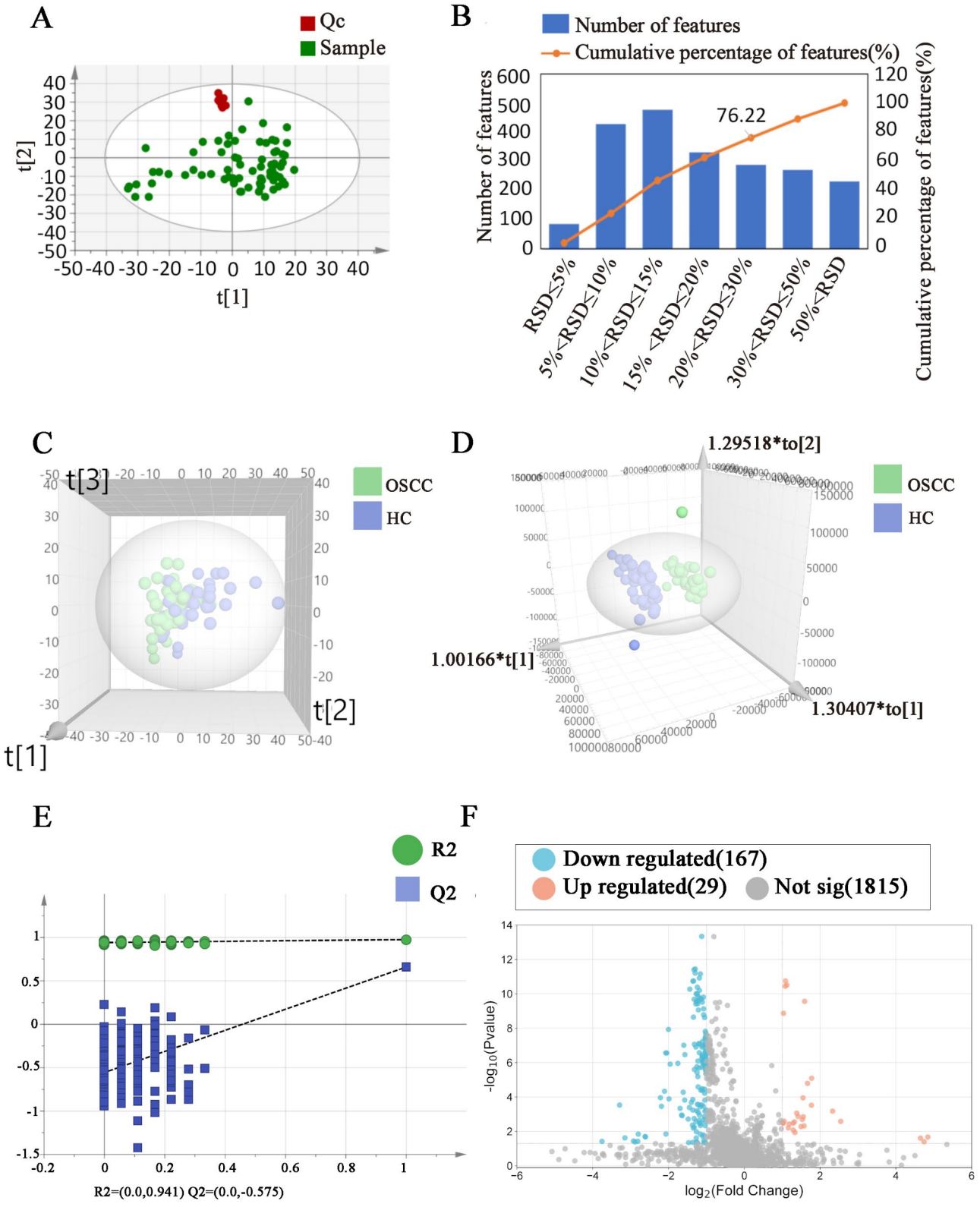

Fig. 3 Differences in salivary metabolic profiles between OSCC and HC groups. **A** Principal component analysis (PCA) diagram of QC and all saliva samples in positive ion mode; **B** Relative standard deviation (RSD) distribution display diagram of QC sample characteristics; **C** OSCC group and HC group of saliva samples in positive ion mode Principal component analysis (PCA) diagram; **D** Orthogonal partial least squares discriminant analysis (OPLS-DA) 3D score diagram of OSCC group and HC group in positive ion mode of saliva samples; **E** OSCC group and HC group in positive ion mode Permutation analysis diagram of 200 repetitions of permutation test in mode; **F** Volcano plot of OSCC group and HC group in positive ion mode

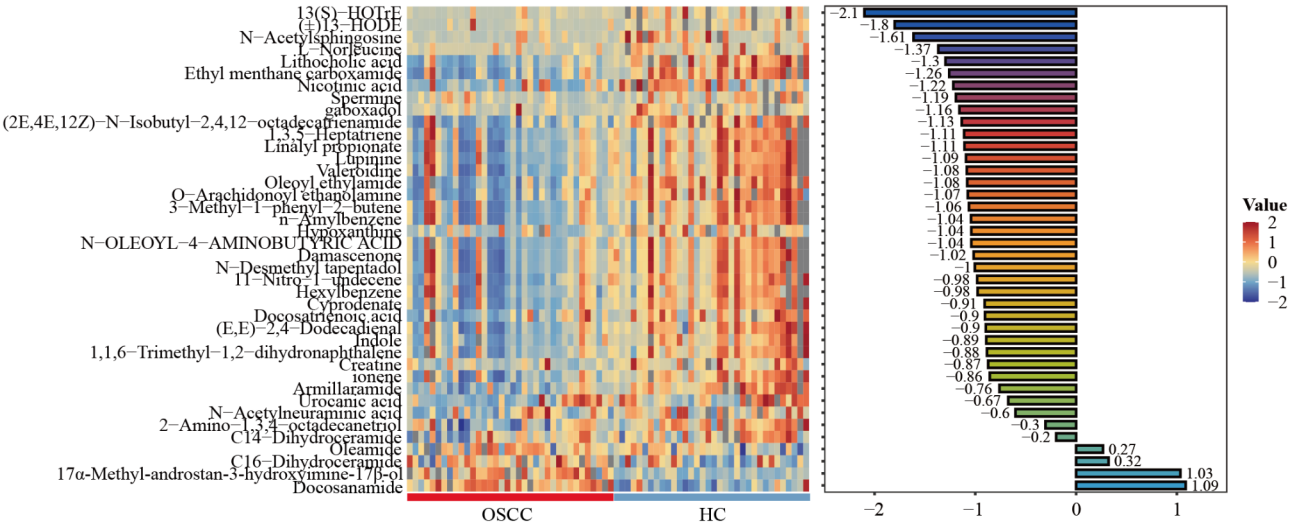

Fig. 4 Heatmap of the distribution of significant differential metabolites in saliva of the OSCC and HC groups. The red and blue colours represent the increase and decrease of differential metabolite levels in the OSCC group compared with the HC group, respectively, with the rows representing metabolite data and the columns representing subjects; the right bar graph represents the multiplicity of differences in the expression of differential metabolites in the OSCC group compared with the HC group, and the values are logarithmic values of differential metabolite ratios, with Value > 0 representing that the metabolite was up-regulated in the OSCC group, and Value < 0 representing that the metabolite was down-regulated in the OSCC group

and metabolites at different microbiota taxonomic levels (Fig. 7A-C), and the tryptophan metabolic pathway was an important metabolic pathway associated with OSCC. Indole and *Pseudomonadota* were the metabolic reactions of this pathway (R00673) metabolites and primary gates (Fig. 7A). The phenylalanine, tyrosine, and tryptophan biosynthesis pathway (ko00400) is another important metabolic pathway associated with OSCC, which involves 2 metabolic reactions (R00674 and R02340) (Fig. 7B, C), and, again, Indole and *Pseudomonadota* are the metabolites and primary gates of two metabolic reactions of this pathway. We subsequently constructed a linear network diagram of microbiome versus metabolites under the microbial metabolic pathway; at the phylum level, five microbiota taxa were closely associated with Indole in the biosynthetic pathway for phenylalanine, tyrosine, and tryptophan (ko00400), and two microbiota taxa were positively correlated with this metabolite (Fig. 8A). At the genus level, 64 microbiota taxa were closely associated with Indole in the tryptophan metabolic pathway (ko00380), and the biosynthetic pathway for phenylalanine, tyrosine, and tryptophan (ko00400) and 28 microbiota taxa were positively correlated with this metabolite (Fig. 8B). This suggests the presence of varying degrees of dysbiosis and metabolite disruption in the OSCC oral cavity and reveals many close links between the oral microbiome and metabolites.

To further analyse the correlation between differential bacterial groups and group-specific metabolites, we performed Spearman correlation analyses between the nine differential bacteria obtained by LEfSe analysis at the genus level and the six differentially abundant metabolites analysed retrospectively on the Metorigin platform for both groups (Fig. 9A). The results revealed that *Capnocytophaga* was negatively correlated with Spermine and Indole (correlation coefficient r < -0.3), whereas there was a significant negative correlation between N-acetylneuraminic acid and *Pseudoalteromonas* and *Vibrio* (correlation coefficient r < -0.4). We subsequently correlated these six colony-specific metabolites with clinical characteristics, such as smoking history and betel nut chewing history (Fig. 9B). The results revealed a significant negative correlation between Oleamide levels and time to disease progression (r = -0.49, P = 0.002).

Discussion

OSCC is a common type of oral cancer. It is characterised by high aggressiveness and the ability to develop lymph node metastases at an early stage. Treatment of cancer focuses on surgical resection, which is usually combined with radiotherapy and chemotherapy [32]. However, current treatment options have not yet achieved the desired therapeutic effect. Therefore, investigating the role of the oral microenvironment in oral carcinogenesis would be beneficial for the prevention and treatment of oral cancer and improve patient prognosis. In this study, we initially conducted a comprehensive comparative analysis of the microbiota and metabolic profiles associated with OSCC.

In the microbiomics study, the Simpson index of the OSCC group was significantly greater than that of the HC group (P < 0.05), and the β diversity showed a significant between-group difference, which is consistent with previous studies [33] and suggests that alterations in the oral microenvironment in cancer states may lead to a

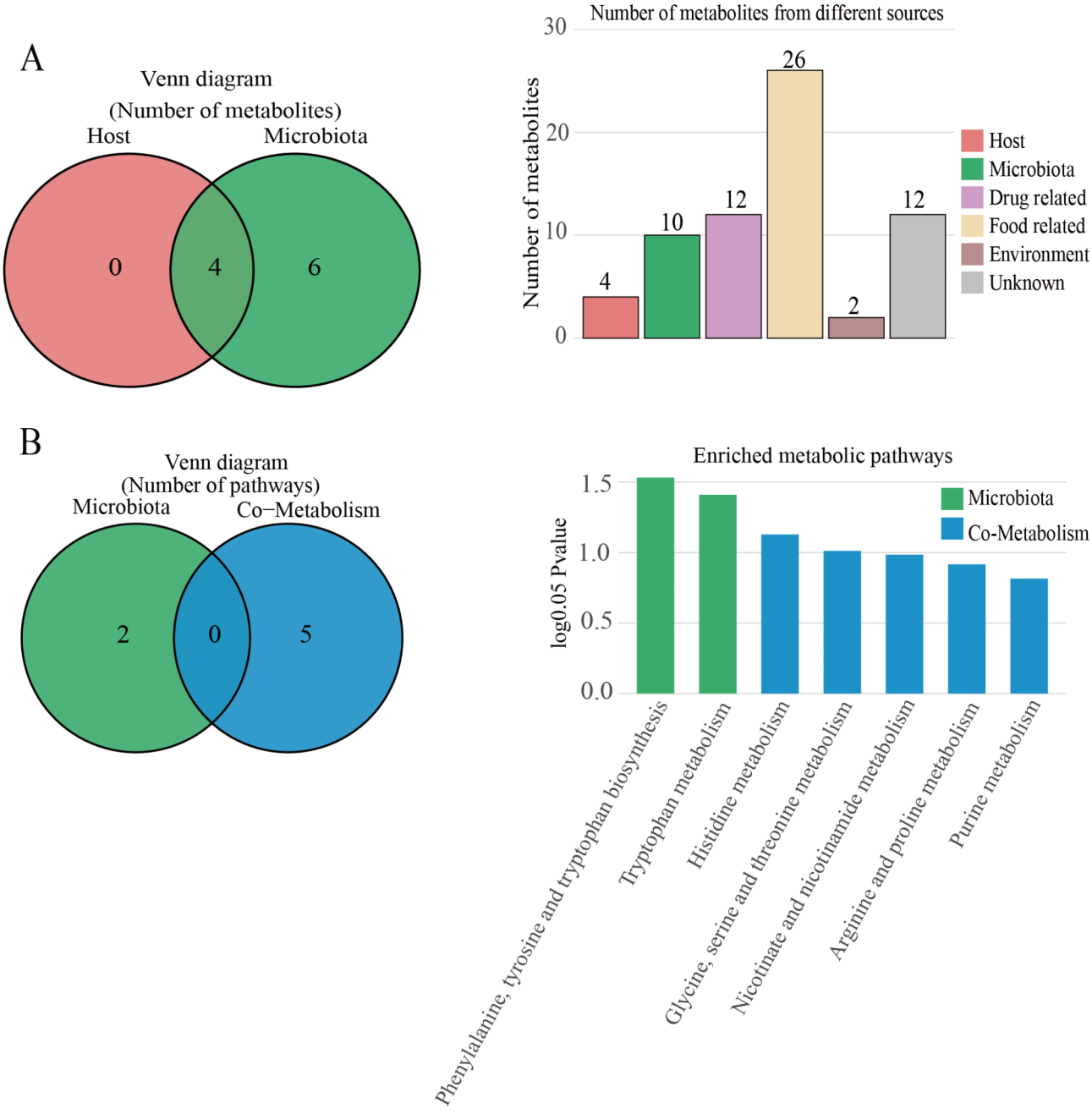

Fig. 5 MetOrigin-based differential metabolite traceability analysis and metabolic pathway enrichment analysis **A** Traceability Wayne plots and histograms of differential metabolites in OSCC and HC groups; **B** Wayne plots and histograms of metabolic pathway enrichment analysis of differential metabolites

decrease in microbiome diversity. Specifically, the cancer-associated microenvironment may affect the composition and diversity of the microbiome through inflammatory responses or immune suppression [34]. These alterations may play important roles in the pathogenesis of oral cancer. The oral microbiota is one of the most complex microbial communities in the human body, and many national and international studies have reported associations between ecological dysregulation and OSCC development [35–38]. However, the results vary widely from study to study. Li [33] et al. reported that the OSCC group was significantly enriched in Bacteroidetes at the phylum level and Prevotella and Peptostreptococcus at the genus level compared with precancerous lesions and healthy controls, but the present study revealed that Prevotella at the genus level was significantly enriched in the HC group. However, the above study used macrogenome sequencing to identify oral salivary microorganisms,

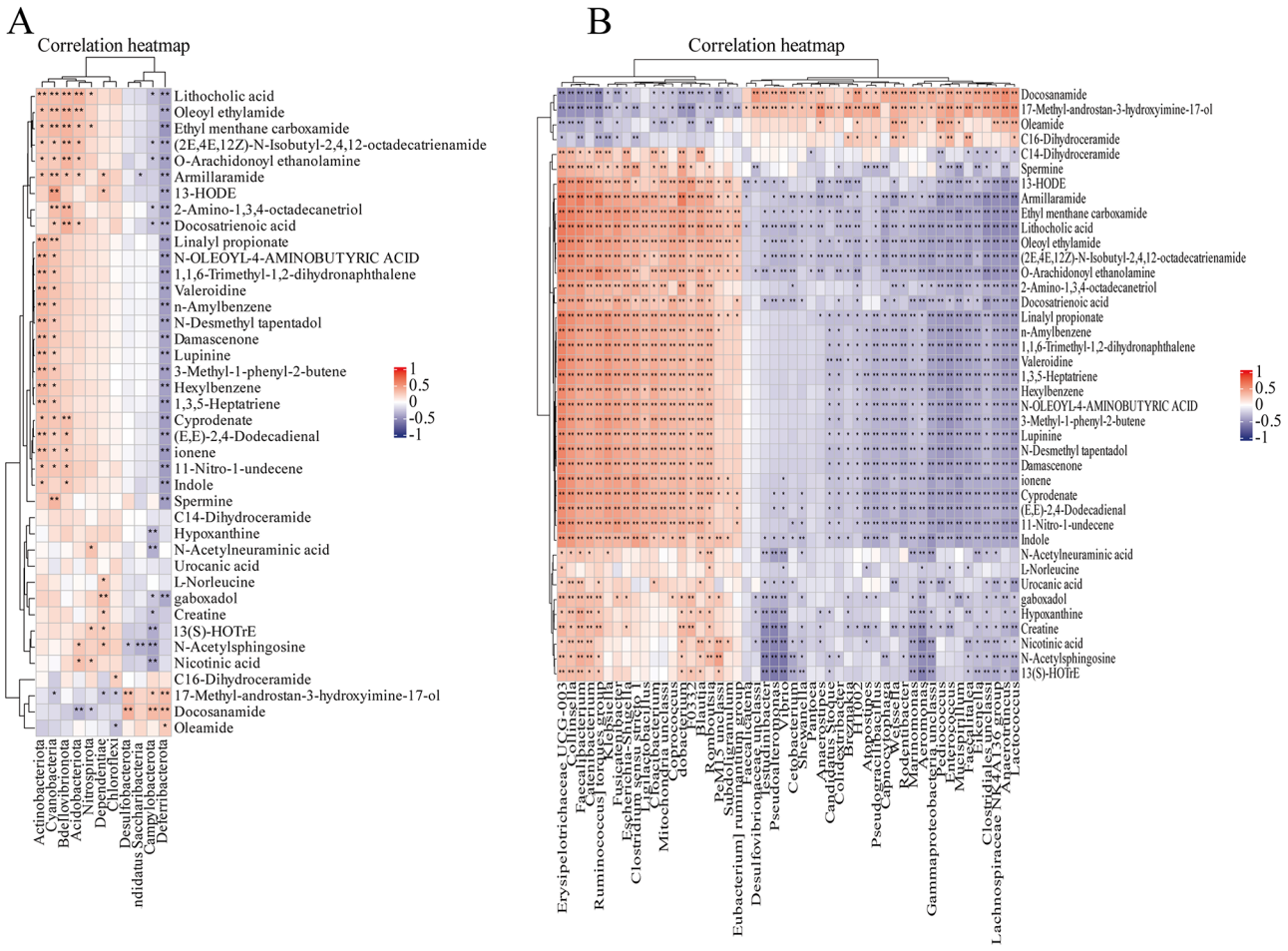

Fig. 6 Heatmap of correlation between differential bacteria and differential metabolites **A** Heatmap of correlation between differential bacteria and differential metabolites at the gate level between OSCC group and HC group; **B** Heatmap of correlation between differential bacteria and differential metabolites at the genus level between OSCC group and HC group. Red represents positive correlation and blue represents negative correlation, the stronger the correlation, the darker the colour. *: $P < 0.05$, **;$P < 0.01$

which is different from the 16 S rDNA gene sequencing technique of the present study. Second, the authors of the above study selected the saliva of only 10 OSCC patients for testing, which may have led to a large random error, whereas the salivary bacterial microbiome characteristics of the 40 OSCC patients in the present study may be more representative.

In our study, the *genera Capnocytophaga*, *Aggregatibacter*, and *Moraxella* were significantly increased at the genus level in the OSCC group. This finding is consistent with the findings of Takahashi and Alejandro, who confirmed that *Capnocytophaga* is a potential tumor promoter in OSCC, which can promote EMT(epithelial-to-mesenchymal transition)-ediated invasion and migration of OSCC cells [39–41]. Several scholars have suggested that *Capnocytophaga* is a potential microbiome diagnostic marker for oral cancer [42, 43]. On the basis of the Spearman correlation coefficient (r < -0.3) of *Capnocytophaga* with spermine and Indole, which was negatively correlated, and combined with the changes in the contents of all three compounds in the oral saliva of the OSCC group, we hypothesised that *Capnocytophaga* might promote OSCC occurrence and development. *Aggregatibacter* is a gram-negative coccobacillus normally found in the oral cavity and upper respiratory tract of humans. *Aggregatibacter actinomycetemcomitans (Aa)* and *Aggregatibacter aphrophilus* are considered the causative agents of periodontitis and infective endocarditis. Aa is also thought to be closely associated with aggressive periodontitis [44], and more recently [45], through in vitro cell experiments, Mark et al. revealed that extracellular vesicles of *Aa* have potential antitumour effects on oral cancer. These studies suggest that *Aggregatibacter* abundance is strongly associated with the development of OSCC. On the other hand, the *genus Streptococcus* was less enriched in the OSCC group than in the healthy group. In 2020, researchers reported that *Aggregatibacter Streptococcus* may serve as a noninvasive biomarker for

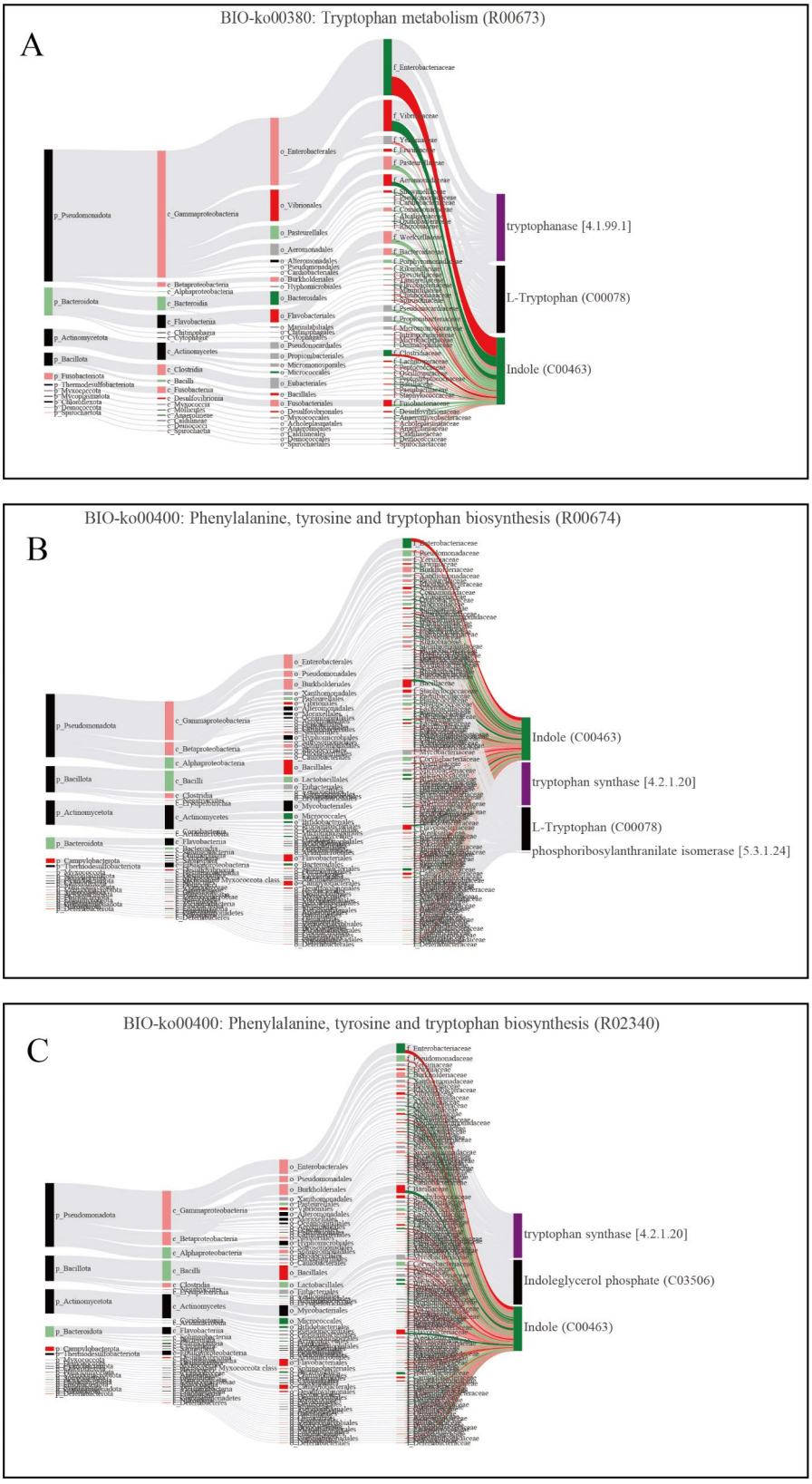

Fig. 7 (See legend on next page.)

(See figure on previous page.)

Fig. 7 BIO-Sankey network diagram of biota-specific metabolic pathways **A** Metabolic pathway of tryptophan (BIO-ko00380); **B** Metabolic reactions (R00674) of the biosynthetic pathway of phenylalanine, tyrosine and tryptophan (BIO-ko00400); **C** Metabolic reactions (R02340) of the biosynthetic pathway of alanine, tyrosine and tryptophan (BIO- ko00400) metabolic reactions (R02340). Dark red (or dark green) bars indicate microorganisms or metabolites significantly elevated (or reduced) in the OSCC group (FC > 1 or FC < 1, $P < 0.05$); light red (or light green) bars indicate microorganisms or metabolites elevated (or reduced) in the OSCC group (FC > 1 or FC < 1, $P \geq 0.05$); and black bands indicate microorganisms or metabolites in the reference database; Purple bands indicate metabolic enzymes; dark red (or green) curved bands indicate statistically significant positive (or negative) correlations (Spearman's correlation test; R > or $R < 0$, $P < 0.05$); light red (or green) bands indicate statistically non-significant positive (or negative) correlations (Spearman's correlation test; R > or $R < 0$, $P \geq 0.05$); light grey bands indicate The correlation analysis was done based on the MetOrigin platform

oropharyngeal cancer [46]. A study of 197 participants with OSCC in Taiwan by Yang [47] et al. revealed that the relative *Streptococcus* abundance decreased with cancer progression and that *Streptococcus* levels were negatively correlated with OSCC progression. These findings support the potential pathogenic role of microbial communities in oral cancer and suggest that specific microbiome may serve as therapeutic targets.

A total of six bacterial-specific metabolites with significant differences were obtained in this study. Spermine is a polyamine metabolite, and elevated levels of polyamines are necessary for tumor transformation and progression [48]. The present study also demonstrated a significant downregulation of salivary levels of spermine in the OSCC group compared with the normal control group in oral cancers. Indole is an important intermediate in the metabolism of tryptophan. Indole exerts an oncogenic effect on prostate cancer cells, colorectal cancer, breast cancer, and childhood glioblastoma and can be used as a diagnostic marker for detecting prostate cancer [49–54]. Ishikaw et al. noted that patients with OSCC had higher levels of indole-3-acetate in their saliva compared to patients with benign lichen planus [55]. But in this study, Indole was significantly reduced in the oral saliva of the OSCC group, which also suggested that Indole might have an inhibitory effect on OSCC, while the Sankey diagram and linear network diagram of this study demonstrated three metabolic mechanisms involving the metabolites of the six microbiome, all of which involve Indole. Moreover, linear network diagrams at the phylum and genus levels revealed that Indole was located in the differential microbiome at the center of the correlation between differentially abundant metabolites. However, the mechanism of Indole and its derivatives in the development of oral squamous cell carcinoma (OSCC) has not been investigated. In addition to this, Balwinder Kaur et al. detailed that the inhibitory effect of indole on human cancer cells has been demonstrated in the development of new anticancer drugs [56]. Indole and its derivatives, as well as the bacteria closely associated with them, may provide a novel research perspective on the occurrence and development of oral squamous cell carcinoma (OSCC), and in-depth exploration of the interactions of indole and its derivatives with the oral microbiota may reveal mechanisms that have not yet been fully recognized in the pathogenesis of OSCC.N-acetylneuraminic acid is a type of salivary acid (sialic acid), which is a special class of monosaccharide among sugar metabolites. N-acetylneuraminic acid levels in the serum and saliva of OSCC patients increase significantly with increasing histopathological grade, and it has been proposed as a biomarker for the diagnosis of OSCC [57–59]. However, our results revealed that N-acetylneuraminic acid levels in the oral cavity were significantly lower in the OSCC group than in the HC group. This may be due to the differences in the samples used in different studies and the different methods of analysis used in the studies; however, in the present study, the liquid chromatography method used was more capable of saliva separation and could detect changes in N-acetylneuraminic acid in the salivary acid in a relatively fine way. 13-HODE is a lipid metabolite that is a product generated by the oxidation of linoleic acid (linoleic acid) through the lipoxygenase (LOX) pathway.13-HODE can inhibit the proliferation of human colon cancer cells [60]. In the present study, the significant reduction in 13-HODE in the oral cavity of the OSCC group may suggest that 13-HODE also has some inhibitory effect on OSCC, but the exact mechanism is not clear. Oleamide is a fatty acid amide among lipid metabolites, and studies have reported that oleamide analogues, including linoleamide, can cause apoptosis in human bladder, urinary and breast cancer (BCa) cells and have antiproliferative, antiangiogenic and antimetastatic effects. In this study, we detected a significant decrease in Oleamide levels in the OSCC group, which seems to suggest that Oleamide may also have a role in OSCC cells. Moreover, on the basis of the correlation analysis of differentially abundant metabolites with clinical features, the abundance of oleamide in the oral saliva of the OSCC group was negatively correlated with the time of onset of clinical symptoms in the OSCC participants, which verified this effect. Damascenone belongs to a group of carotenoid degradation products, and damascenone and its derivatives have been reported to inhibit Raw 264.7 lipopolysaccharide-induced nitric oxide synthase activity in macrophages and reduce the levels of inflammatory mediators, thereby preventing tumor development [61]. The level of damascenone in the oral cavity of the OSCC patients in the present study was significantly lower than normal, further suggesting that damascenone may have some inhibitory effect on the development of OSCC.

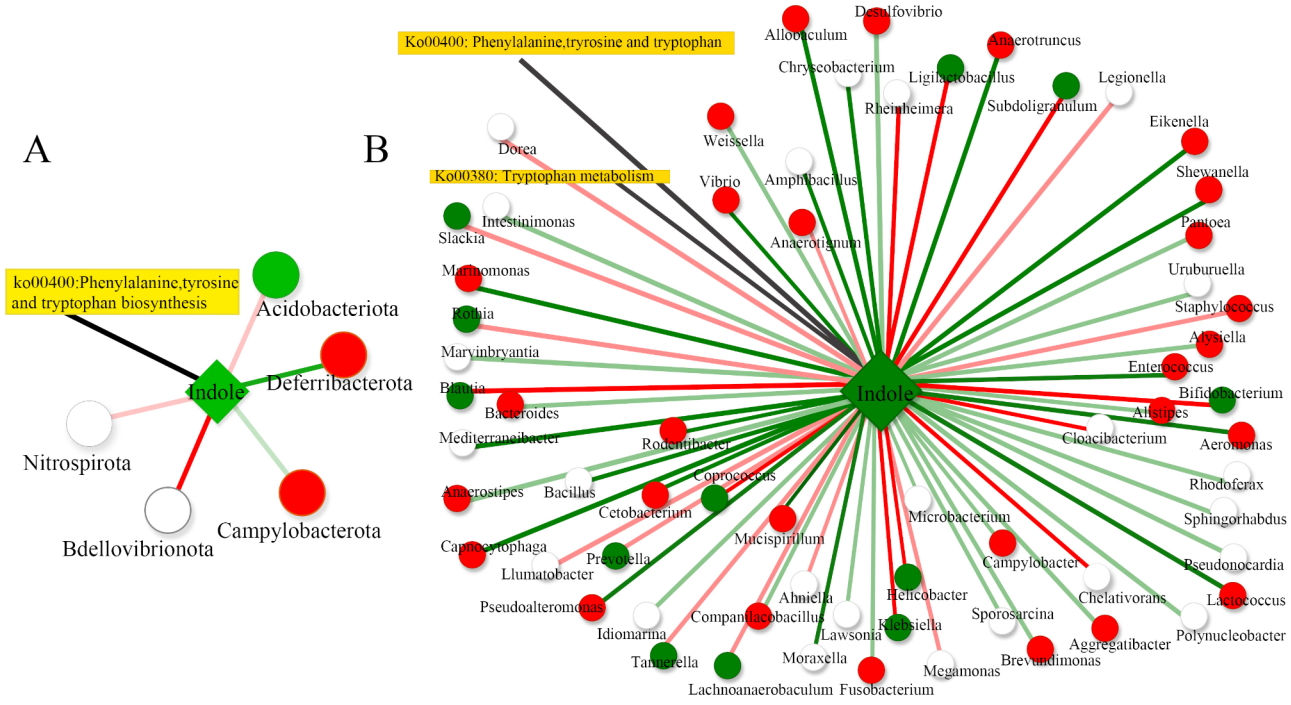

Fig. 8 Linear network diagram of differential microbiome with differential metabolites **A** linear network diagram of differential microbiome with metabolites at the phylum level; **B** linear network diagram of differential microbiome with metabolites at the genus level. Diamonds and dots indicate associated metabolites and microorganisms, respectively. Red (or green) nodes indicate significantly higher (or lower) OSCC group of microbiome. Red (or green) connecting lines indicate positive (or negative) correlations between microorganisms and metabolites; correlation analyses were done based on the MetOrigin platform

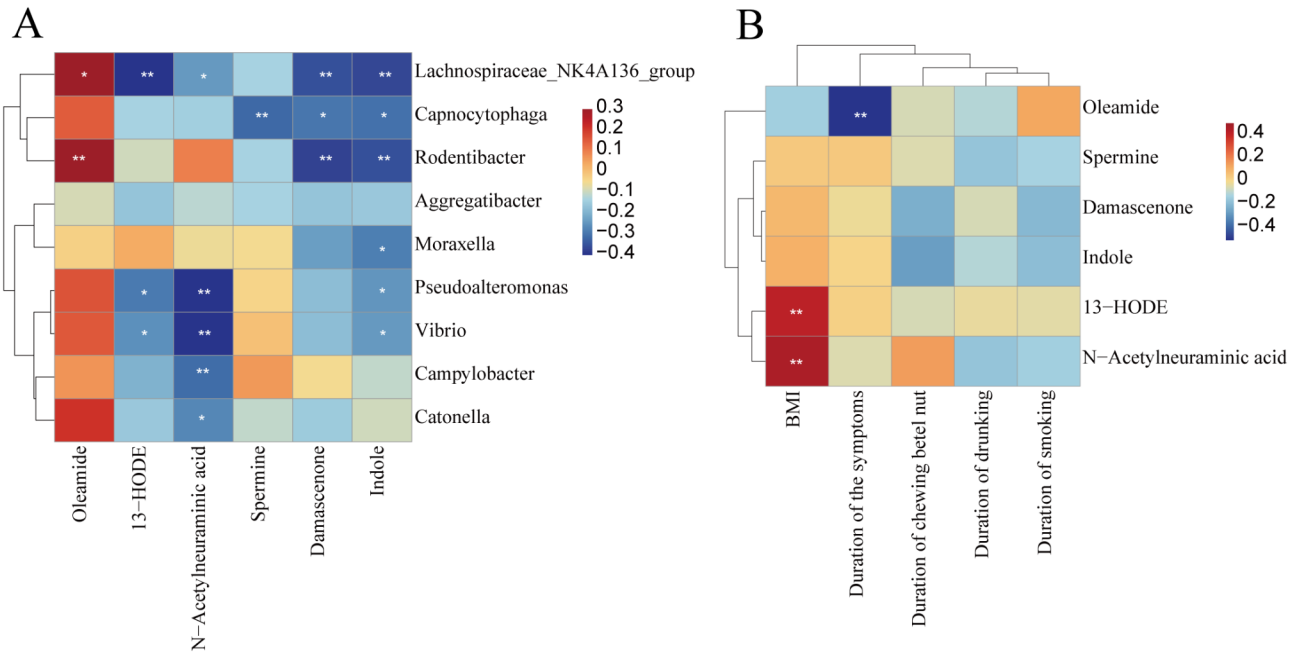

Fig. 9 Correlation analysis between characteristic differential organisms, colony-specific metabolites and clinical features in OSCC groups. **A** Spearman correlation analysis heatmap between genus-level differential organisms obtained from LEfSe analysis and colony-specific metabolites analysed retrospectively on Metorigin platform; **B** Spearman correlation analysis heatmap between colony-specific metabolites and clinical characteristics of OSCC participants. Spearman correlation analysis heatmap between colony-specific metabolites and clinical characteristics of OSCC participants. Red represents positive correlation and blue represents negative correlation, the stronger the correlation, the darker the colour. *:$P < 0.05$, **; $P < 0.01$

In this study, we found that these six differentially abundant metabolites associated with the colony involved two metabolic pathways ($P<0.05$) through the Metorign platform: the phenylalanine, tyrosine and tryptophan biosynthesis pathways and the tryptophan metabolism pathway. Phenylalanine, tyrosine and tryptophan are three important aromatic amino acids, and their biosynthetic pathways play key roles in many biological processes, including protein synthesis, metabolic regulation and signalling. Aromatic amino acid metabolic pathways may be altered in OSCC cells to support tumor growth and progression. Metabolic reprogramming is one of the main hallmarks of malignancy, where tumor cells promote growth, proliferation and immune evasion by altering their metabolism, microenvironment and immune cell function [62]. All six differentially abundant metabolites associated with these two metabolic pathways were significantly downregulated in the oral saliva of the OSCC group. The significant correlation between specific bacterial taxa and specific metabolites suggests that these microorganisms may influence the course of oral cancer through metabolic pathways. These findings provide a basis for further investigation of the microbe–metabolite–disease axis and may provide clues for the development of new therapeutic strategies.

Conclusion

In this study, we fully explored the changes of OSCC salivary microorganisms and metabolites at the microbiome and metabolomics levels, and screened out the differential flora represented by Capnocytophaga bacteria, and a variety of metabolites represented by indoles. The potential connection between the two was also discovered through correlation analysis, which provided a theoretical basis for the oral flora to influence the occurrence and development of OSCC through the secretion of metabolites.

Abbreviations

OSCC	Oral squamous cell carcinoma
HC	Healthy control
LC-MS	Liquid Chromatography-Mass Spectrometry
HPV	Human papillomavirus
OSCC	Oral squamous cell carcinoma
CTAB	Cetyl Trimethyl Ammonium Bromide
QIIME	Quantitative Insights Into Microbial Ecology
OUT	Operational Taxonomic Unit
PCA	Principal Component Analysis
OPLS-DA	Orthogonal Partial Least Squares Discriminant Analysis
QC	Quality Control
BMI	Body Mass Index
PCoA	Principal Coordinates Analysis
LEfSe	LDA Effect Size
LDA	Linear Discriminant Analysis
RSD	Relative Standard Deviation
VIP	Variable Importance in Projection

Supplementary Information

The online version contains supplementary material available at https://doi.org/10.1186/s12885-025-13680-5.

Supplementary Material 1

Supplementary Material 2

Supplementary Material 3

Supplementary Material 4

Supplementary Material 5

Acknowledgements

The authors thank all of the participants who recruited patients in this study.

Author contributions

KW, YM, and JX: Formal analysis; writing-original draft; writing-review and editing. HZ, LX, and YS: Methodology; writing-review and editing. RC and ZS: Investigation. QS: Conceptualization; funding acquisition; formal analysis; writing-review and editing. All authors read and approved the final manuscript.

Funding

Talent Training Project in Henan Province (GCC2025054); Graduate Student Independent Innovation Project of Zhengzhou University (20240349); Colleges and Universities in Henan Province Key Scientific Research Project Funding Scheme (24A320056); Zhengzhou University Young Teacher Training Fund (JC23862075); Young and Middle-aged Health Discipline Leader of Henan Health Commission (HNSWJW-2022016); Key Research and Development and Promotion (Science and Technology Research) Project of Henan Provincial Department of Science and Technology (212102310592).

Data availability

No datasets were generated or analysed during the current study.

Declarations

Ethics approval and consent to participate

The study was approved by the Ethics Committee of the First Affiliated Hospital of Zhengzhou University (Approval No.: 2019-KY-305), and implemented following the Declaration of Helsinki.

Consent for publication

Not Applicable.

Competing interests

The authors declare no competing interests.

Received: 22 November 2024 / Accepted: 6 February 2025
Published online: 04 April 2025

References

1. Mody M D, Rocco J W, Yom SS, et al. Head neck cancer [J] Lancet. 2021;398(10318):2289–99.
2. Bray F, Laversanne M. Global cancer statistics 2022: GLOBOCAN estimates of incidence and mortality worldwide for 36 cancers in 185 countries [J]. CA Cancer J Clin. 2024;74(3):229–63.
3. Wang D, Gao J, Zhao C, et al. Cyclin G2 inhibits oral squamous cell carcinoma growth and metastasis by binding to IGFBP3 and regulating the FAK-SRC-STAT signaling pathway [J]. Front Oncol. 2020;10:560572.
4. Johnson D E Burtnessb, Leemans C R, et al. Head and neck squamous cell carcinoma [J]. Nat Rev Dis Primers. 2020;6(1):92.
5. Shigeishi H. Association between human papillomavirus and oral cancer: a literature review [J]. Int J Clin Oncol. 2023;28(8):982–9.
6. Shetty SS, Vishal RAO U. 8 S in oral cancer [J]. Oral Oncol. 2019;88:27–8.

7. Yang Z, Sun P, Dahlstrom K R, et al. Joint effect of human papillomavirus exposure, smoking and alcohol on risk of oral squamous cell carcinoma [J]. BMC Cancer. 2023;23(1):457.
8. Stasiewicz M, KarpiŃSKI TM. The oral microbiota and its role in carcinogenesis [J]. Semin Cancer Biol. 2022;86(Pt 3):633–42.
9. Li R, Xiao L, Gong T, et al. Role of oral microbiome in oral oncogenesis, tumor progression, and metastasis [J]. Mol Oral Microbiol. 2023;38(1):9–22.
10. Liao O, Ye G, Du Q, et al. Gastric microbiota in gastric cancer and precancerous stages: mechanisms of carcinogenesis and clinical value [J]. Helicobacter. 2023;28(3):e12964.
11. SAlvatori S, Marafini I, Laudisi F et al. Helicobacter pylori and gastric Cancer: pathogenetic mechanisms [J]. Int J Mol Sci, 2023, 24(3).
12. Tuominen H. Oral microbiota and Cancer Development [J]. Pathobiology. 2021;88(2):116–26.
13. Nieminen M T, Listyarifah D, Hagström J, et al. Treponema denticola chymotrypsin-like proteinase may contribute to orodigestive carcinogenesis through immunomodulation [J]. Br J Cancer. 2018;118(3):428–34.
14. Rodriguez R M, Hernandez B Y, Menor M, et al. The landscape of bacterial presence in tumor and adjacent normal tissue across 9 major cancer types using TCGA exome sequencing [J]. Comput Struct Biotechnol J. 2020;18:631–41.
15. Vila T, Sultan A S, Montelongo-Jauregui D et al. Oral candidiasis: a disease of opportunity [J]. J Fungi (Basel), 2020, 6(1).
16. Fonsêca TC, Jural L A, Marañón-váSquez GA, et al. Global prevalence of human papillomavirus-related oral and oropharyngeal squamous cell carcinomas: a systematic review and meta-analysis [J]. Clin Oral Investig. 2023;28(1):62.
17. Nyssa C, Camila Azevedo A, Ravid S et al. Microbiome and cancer [J]. Cancer Cell, 2021.
18. Zhenrun J Z, Yen-Chih W, Xinglin Y et al. Chemical Reporters for Exploring Microbiology and Microbiota Mechanisms [J]. ChemBioChem, 2019.
19. Porter SR. Oral malodour (halitosis) [J]. BMJ. 2006;333(7569):632–5.
20. Katarzyna H, Marcelina M J, Zuzanna ŁUCJA B et al. The role of oral microbiota in Intra-oral Halitosis [J]. J Clin Med, 2020.
21. Claudia L, Vinay P, Christiane P, et al. The Saliva Metabolome in Association to oral health status [J]. Journal of Dental Research; 2019.
22. Alexander G, Guy C, Po-Wah S. Salivary Metabolomics: From Diagnostic Biomarker Discovery to Investigating Biological Function [J]. Metabolites, 2020.
23. Torresano L, Nuevo-Tapioles C, Santacatterina F, et al. Metabolic reprogramming and disease progression in cancer patients [J]. Biochim Biophys Acta Mol Basis Dis. 2020;1866(5):165721.
24. Halma M T J, Tuszynski J A. Marik P E. Cancer Metabolism as a therapeutic target and review of interventions [J]. Nutrients, 2023, 15(19).
25. Oyeyemi B F, Kaur U S, Paramraj A, et al. Microbiome analysis of saliva from oral squamous cell carcinoma (OSCC) patients and tobacco abusers with potential biomarkers for oral cancer screening [J]. Heliyon. 2023;9(11):e21773.
26. Zhou Y, Liu Z. Saliva biomarkers in oral disease [J]. Clin Chim Acta. 2023;548:117503.
27. Mehterov N, Vladimirov B, Sacconi A et al. Salivary miR-30c-5p as potential biomarker for detection of oral squamous cell carcinoma [J]. Biomedicines, 2021, 9(9).
28. Caporaso Jg, Justin K, Jesse S et al. QIIME allows analysis of high-throughput community sequencing data [J]. Nat Methods, 2010.
29. Morgan N P Paramvird, Adam P A. FastTree 2 – Approximately Maximum-Likelihood Trees for Large Alignments [J]. Plos One, 2010.
30. Huang C, YI X. Disordered cutaneous microbiota in systemic lupus erythematosus [J]. J Autoimmun. 2020;108:102391.
31. Segata N, Izard J, Waldron L, et al. Metagenomic biomarker discovery and explanation [J]. Genome Biol. 2011;12(6):R60.
32. Tan Y, Wang Z, XU M, et al. Oral squamous cell carcinomas: state of the field and emerging directions [J]. Int J Oral Sci. 2023;15(1):44.
33. Li Z, Chen G, Wang P, et al. Alterations of the oral microbiota profiles in Chinese patient with oral Cancer [J]. Front Cell Infect Microbiol. 2021;11:780067.
34. Bishehsari F, Voigt R M Keshavarziana. Circadian rhythms and the gut microbiota: from the metabolic syndrome to cancer [J]. Nat Rev Endocrinol. 2020;16(12):731–9.
35. Lindemann A, Takahashi H, Patel A A, et al. Targeting the DNA damage response in OSCC with TP53 mutations [J]. J Dent Res. 2018;97(6):635–44.
36. Yu X, Shi Y, Yuan R, et al. Microbial dysbiosis in oral squamous cell carcinoma: a systematic review and meta-analysis [J]. Heliyon. 2023;9(2):e13198.
37. Frank D N, Qiu Y, Cao Y, et al. A dysbiotic microbiome promotes head and neck squamous cell carcinoma [J]. Oncogene. 2022;41(9):1269–80.
38. Zhang Z, Feng Q, Li M, et al. Age-Related Cancer-Associated Microbiota potentially promotes oral squamous cell Cancer tumorigenesis by distinct mechanisms [J]. Front Microbiol. 2022;13:852566.
39. Takahashi Y, Park J, Hosomi K, et al. Analysis of oral microbiota in Japanese oral cancer patients using 16S rRNA sequencing [J]. J Oral Biosci. 2019;61(2):120–8.
40. Herreros-Pomares A, Hervás D, Bagan-Debón L et al. On the oral microbiome of oral potentially malignant and malignant disorders: Dysbiosis, loss of Diversity, and Pathogens Enrichment [J]. Int J Mol Sci, 2023, 24(4).
41. Zhu W, Shen W, Wang J, et al. Capnocytophaga gingivalis is a potential tumor promotor in oral cancer [J]. Oral Dis. 2024;30(2):353–62.
42. Mager D L, Haffajee A D, Devlin P M, et al. The salivary microbiota as a diagnostic indicator of oral cancer: a descriptive, non-randomized study of cancer-free and oral squamous cell carcinoma subjects [J]. J Transl Med. 2005;3:27.
43. Saxena R, Prasoodanan P K V Guptasv, et al. Assessing the Effect of Smokeless Tobacco Consumption on oral microbiome in healthy and oral Cancer patients [J]. Front Cell Infect Microbiol. 2022;12:841465.
44. Lindholm M, Min Aung K, Nyunt Wai S, et al. Role of OmpA1 and OmpA2 in Aggregatibacter actinomycetemcomitans and Aggregatibacter aphrophilus serum resistance [J]. J Oral Microbiol. 2019;11(1):1536192.
45. Metsäniitty M, Hasnat S, Öhman C, et al. Extracellular vesicles from Aggregatibacter actinomycetemcomitans exhibit potential antitumorigenic effects in oral cancer: a comparative in vitro study [J]. Arch Microbiol. 2024;206(6):244.
46. Mukta P, Avdhesh K, Tashnin R, et al. Alterations of salivary microbial community associated with oropharyngeal and hypopharyngeal squamous cell carcinoma patients [J]. Archives of Microbiology; 2019.
47. Chao-Ping Y, Yuan-Ming Y, Haiying Y, et al. Oral Microbiota Community Dynamics Associated with oral squamous cell carcinoma staging [J]. Frontiers in Microbiology; 2018.
48. Murray-Stewart T R, Woster P M, Casero R A JR. Targeting polyamine metabolism for cancer therapy and prevention [J]. Biochem J. 2016;473(19):2937–53.
49. Xiaoling Z, Christina M J, Tran Quoc L et al. Feasibility of detecting prostate Cancer by Ultraperformance Liquid Chromatography–Mass Spectrometry serum metabolomics [J]. J Proteome Res, 2014.
50. Li Z, Ding B, Ali M R K et al. Dual effect of tryptamine on prostate Cancer cell growth regulation: a pilot study [J]. Int J Mol Sci, 2022, 23(19).
51. Zhao J, Carbone J, Farruggia G et al. Synthesis and antiproliferative activity against Cancer cells of Indole-Aryl-Amide derivatives [J]. Molecules, 2022, 28(1).
52. Liu Y, Pei Z, Pan T, et al. Indole metabolites and colorectal cancer: gut microbial tryptophan metabolism, host gut microbiome biomarkers, and potential intervention mechanisms [J]. Microbiol Res. 2023;272:127392.
53. Alberto Z, Richard T, Sara N et al. Trabectedin and indole-3-carbinol combination in heavily pretreated metastatic breast cancer: results of a pilot clinical study [J]. J Clin Oncol, 2014.
54. Shahinda S R A, Amreena S, Anders W B, et al. Synthesis and antitumour evaluation of indole-2-carboxamides against paediatric brain cancer cells [J]. RSC medicinal chemistry; 2021.
55. Ishikawa S, Sugimoto M, Edamatsu K, et al. Discrimination of oral squamous cell carcinoma from oral lichen planus by salivary metabolomics [J]. Oral Dis. 2020;26(1):35–42.
56. Kaur B, Venugopal S. Recent developments in the synthesis and anticancer activity of Indole and its derivatives [J]. Curr Org Synth. 2023;20(4):376–94.
57. Rajaram S, Danasekaran B P, Venkatachalapathy R, et al. N-acetylneuraminic acid: a scrutinizing tool in oral squamous cell carcinoma diagnosis [J]. Dent Res J (Isfahan). 2017;14(4):267–71.
58. Pratibha P, Barsha B. Shubrato B, et al. Estimation of serum and salivary sialic acid level in patients with oral squamous cell carcinoma [J]. Journal of College of Medical Sciences-nepal; 2019.
59. SJ V, SA P et al. VAS E,. Expanding salivary biomarker detection by creating a synthetic neuraminic acid sensor via chimeragenesis [J]. bioRxiv: the preprint server for biology, 2024, null.
60. Jian-Xing C, Li J, Yinqiu W et al. 12/15 lipoxygenase regulation of colorectal tumorigenesis is determined by the relative tumor levels of its metabolite 12-HETE and 13-HODE in animal models [J]. Oncotarget, 2014.

61. Clarissa G, Karin K, Wolfgang H, et al. Identification of 3-hydroxy-β-damascone and related carotenoid-derived aroma compounds as novel potent inducers of Nrf2-mediated phase 2 response with concomitant anti-inflammatory activity [J]. Molecular Nutrition & Food Research; 2009.
62. Claudia P, Ielizaveta G, Daria K et al. Metabolic regulation of prostate cancer heterogeneity and plasticity [J]. Sem Cancer Biol, 2022.

Publisher's note